Wang et al. *Zool. Res.* 2026, 47(1): 88−100
https://doi.org/10.24272/j.issn.2095-8137.2025.319
https://cstr.cn/32248.14.zr.2025.319

ZR | Zoological Research

Article Open Access

Comparative genomics reveals evolutionary signatures of genes associated with jumping in beetles

Wei Wang[1,#], Le Zong[1,#], Jin-Wu He[2], Chu-Yang Mao[2,3], Zhi-Wei Dong[2], Ping-Ping Yang[1], Zheng-Zhong Huang[1], Cong-Qiao Li[1], Wen-Jie Li[1,3], Yong-Ying Ruan[4], Chuan Feng[1,3], Xue-Yan Li[2,3,5,*], Si-Qin Ge[1,3,*]

[1] *State Key Laboratory of Animal Biodiversity Conservation and Integrated Pest Management*, *Institute of Zoology*, *Chinese Academy of Sciences*, *Beijing* 100101, *China*

[2] *State Key Laboratory of Genetic Evolution* & *Animal Models*, *Kunming Institute of Zoology*, *Chinese Academy of Sciences*, *Kunming*, *Yunnan* 650223, *China*

[3] *University of Chinese Academy of Sciences*, *Beijing* 100049, *China*

[4] *Plant Protection Research Center*, *Shenzhen Polytechnic University*, *Shenzhen*, *Guangdong* 518055, *China*

[5] *Yunnan Key Laboratory of Biodiversity Information*, *Kunming Institute of Zoology*, *Chinese Academy of Sciences*, *Kunming*, *Yunnan* 650223, *China*

ABSTRACT

Jumping has independently emerged as an effective escape strategy across multiple beetle lineages (order Coleoptera). Characterization of jumping behavior not only informs the development of bioinspired robotic systems but also advances understanding of adaptive processes and convergent evolution. However, despite extensive behavioral studies in beetles, the genetic mechanisms and evolutionary trajectories underlying this locomotor strategy remain largely unresolved. To elucidate the molecular basis of jumping adaptation and convergent evolution, a comparative genomic analysis was conducted using high-quality assemblies, including one newly generated genome, from jumping beetles representing three families and their non-jumping sister taxa spanning over 200 million years of evolutionary divergence. Genes associated with energy metabolism exhibited extensive signals of rapid evolution and positive selection in jumping beetles, consistent with the elevated energy requirements of explosive locomotion. These observations parallel previous reports linking energy metabolism genes to other high-demand locomotor modes such as flight, suggesting shared molecular signatures across functionally distinct behaviors. Jumping beetles exhibited convergent amino acid substitutions in *bab1*, a regulator of leg disc development, alongside evidence of positive selection and accelerated evolution in the dynein gene *Dnai4* and a significant expansion in copy number of the skeletal muscle gene *Fhl2*. Together, these results implicate both limb morphogenesis and muscle performance genes in the emergence of beetle jumping. This study highlights key genetic mechanisms underlying behavioral innovation and offers novel insights into adaptive convergence in insect locomotion.

Keywords: Jumping locomotion; Adaptive evolution; Molecular convergence; Flea beetle; *Asiophrida xanthospilota*

INTRODUCTION

Jumping behavior has evolved independently across multiple arthropod lineages, reflecting a widespread and convergent locomotor adaptation within this most diverse animal phylum (Chapman, 2013; Furth & Suzuki, 1992; Maulik, 1929). Among arthropods, jumping enables rapid escape from predators and efficient movement across short distances (Chapman, 2013; Nadein & Betz, 2016; Smith & Harrison, 2024). In beetles (Coleoptera), this behavior has arisen in several phylogenetically distinct families, including Chrysomelidae (leaf beetles), Curculionidae (weevils), Buprestidae (jewel beetles), Elateridae (click beetles), and Scirtidae (marsh beetles). These lineages exhibit biomechanical specializations that allow elastic energy storage in modified anatomical structures, often located in either the legs or thorax, enabling rapid energy release during takeoff (Furth & Suzuki, 1992; Nadein & Betz, 2018; Nadein et al., 2022; Ribak & Weihs, 2011). For instance, beetles in Chrysomelidae, Curculionidae, and Buprestidae have independently evolved a specialized

Received: 10 July 2025; Accepted: 21 July 2025; Online: 14 August 2025

Foundation items: This work was supported by the National Natural Science Foundation of China (32270460), Third Xinjiang Scientific Expedition Program (2021xjkk0605), and Yunnan Provincial Science and Technology Department (Talent Project of Yunnan: 202105AC160039)

[#]Authors contributed equally to this work

*Corresponding authors, E-mail: lixy@mail.kiz.ac.cn; gesq@ioz.ac.cn

metafemoral spring apparatus within their legs, providing a striking example of morphological convergence despite deep evolutionary divergence (Furth & Suzuki, 1992). Within Chrysomelidae, flea beetles (Galerucinae: Alticini) have become a prominent model for investigating the biomechanics and evolution of jumping, with research spanning almost a century (Furth & Suzuki, 1992; Ge et al., 2011; Maulik, 1929; Zong et al., 2023).

Flea beetles comprise approximately 10 000 species across 601 genera, nearly all capable of executing powerful jumps (Douglas et al., 2023; Furth et al., 1983). These beetles rank among the most proficient jumpers in the animal kingdom, achieving takeoff distances reaching up to 289 times their body length (Furth et al., 1983; Schmitt, 2004). Jumping has long been recognized as a key adaptation and critical driver of the success of this hyperdiverse group and may be associated with accelerated diversification rates relative to closely related taxa (Ge et al., 2011; Ruan et al., 2020). Recent advances in biomechanical analysis, including three-dimensional (3D) kinematic reconstruction and high-speed videography, have enabled detailed investigation of flea beetle jumping mechanics and have driven the translation of these principles into bioinspired engineering, such as the design of robotic jumping limbs (Nadein & Betz, 2016; Ruan et al., 2020; Zong et al., 2023). However, despite extensive behavioral characterization and technological interest, the genomic architecture underpinning this extreme locomotor specialization remains unknown.

Jumping locomotion, similar to flight, is energetically demanding. Metabolic rate serves as a robust proxy for energy expenditure and shows a positive association with jumping performance in insects (Krasnov et al., 2004). In beetles, the kinetic energy expended per jump is estimated to be 0.2–19.7 μJ in taxa such as flea beetles and jumping weevils (Nadein & Betz, 2016, 2018; Nadein et al., 2022), corresponding to approximately 4–400 trillion adenosine triphosphate (ATP) molecules. However, the true metabolic cost is expected to be considerably higher due to inefficiencies during conversion of chemical energy into mechanical output. Oxidative phosphorylation provides more than 95% of cellular energy in eukaryotes (Erecińska & Wilson, 1982), and genes involved in this pathway have been implicated in the evolution of energetically demanding locomotor modes such as flight (Mitterboeck et al., 2017; Shen et al., 2010). Comparative genomic analyses have revealed many oxidative phosphorylation genes bearing evolutionary signatures of positive selection in flying lineages relative to non-flying relatives, although the extent of such signatures varies across birds, bats, and insects (Mitterboeck et al., 2017; Shen et al., 2010). In contrast to flight, jumping in beetles relies on distinct strategies of energy storage and release, often involving elastic protein-chitin composites rather than carbohydrate- or lipid-based reserves (Betz et al., 2007; Chatterjee & Perrimon, 2021; Furth et al., 1983; Furth & Suzuki, 1992). This mechanistic distinction raises the question of whether jumping beetles exhibit similar signatures of positive selection in energy metabolism-related genes when compared with non-jumping sister taxa. Molecular convergence is widely recognized as a fundamental contributor to phenotypic convergence (Hao et al., 2019; Rosenblum et al., 2014; Stern, 2013; Tong, 2024), and convergent genetic changes have been repeatedly documented in diverse traits, such as echolocation, infrared sensing, dietary specialization, viviparity, and plunge-diving across multiple animal clades through comprehensive comparative genomics (Eastment et al., 2024; Eliason et al., 2023; Hu et al., 2017; Sadanandan et al., 2023; Zhou et al., 2025; Zou et al., 2024). However, whether genome-wide convergent evolution has acted on genes involved in the jumping process—particularly those related to muscle structure—in distantly related beetles remains an open question.

To explore these questions, a chromosome-level genome was *de novo* assembled for the flea beetle *Asiophrida xanthospilota*, a species previously shown to exhibit high-performance jumping, including elevated take-off velocity (Ruan et al., 2020; Yang, 2020) (Figure 1). Comparative genomic analyses were then conducted between *As. xanthospilota* and other high-quality genomes representing jumping beetles, including four species from Chrysomelidae, one species from Curculionidae, and one species from Buprestidae, along with their non-jumping sister taxa (Supplementary Table S1). In jumping lineages, multiple genes associated with energy metabolism exhibited signatures of rapid evolution and positive selection. Additionally, genes involved in limb development and muscle physiology emerged as key genomic components linked to the evolution of this locomotor adaptation. Overall, these findings provide new insights into the molecular basis of adaptation and convergent evolution underlying jumping behavior in beetles.

MATERIALS AND METHODS

Genome sequencing of *As. xanthospilota*

Sample collection and laboratory rearing: Eggs and larvae of *As. xanthospilota* were collected during April and May from 2020 to 2023 at two sites: a village in Yanqing District, Beijing (E115.59°, N40.31°), and a mountainous area within the China National Botanical Garden (E116.12°, N40.00°). Collected specimens were transported to the laboratory and reared to adulthood under controlled conditions: 25°C, 14:10 h light:dark photoperiod, and 55% relative humidity.

Karyotype analysis: Chromosomal karyotyping was performed based on established methods (Wan et al., 2020; Yang et al., 2020), with some modifications. Briefly, gonads from adult males were isolated and subjected to hypotonic treatment of 0.075% sodium citrate for 15–20 min, followed by fixation in methanol/acetic acid (3:1). Samples were softened in 50% acetic acid, spread on glass slides, and stained with 10% Giemsa solution for 2 h. Chromosomes were counted and imaged using a digital camera equipped with a microscope (Nikon, Japan).

DNA extraction and sequencing: Genomic DNA was extracted from pooled whole-body tissues of 30 male and female adults using a DNeasy Blood & Tissue Kit (Qiagen, Germany) and a cetyltrimethylammonium bromide/sodium dodecyl sulfate (CTAB/SDS) protocol. DNA purity and concentration were assessed by measuring optical density (OD) 260/280 ratios (1.8–2.0) and 260/230 ratios (2.0–2.2) using a NanoDrop-2000 spectrophotometer (Thermo Fisher Scientific, USA), alongside quantification with a Qubit fluorometer (Thermo Fisher Scientific, USA) and visualization on 0.75% agarose gels. For short-read sequencing, libraries were constructed and sequenced using the Illumina HiSeq 2000 and MiSeq platforms (Illumina, USA), yielding 102.22 Gb of clean reads after adaptor trimming and quality filtering,

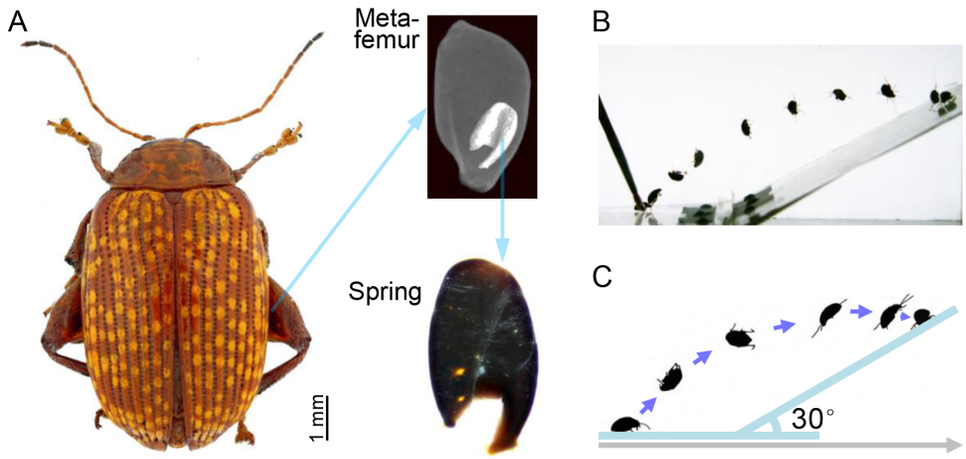

Figure 1 Jumping behavior of the flea beetle *Asiophrida xanthospilota*

A: Adult *As. xanthospilota* (scale bar: 1.0 mm, photo by Ping-Ping Yang) and its jumping "metafemoral spring" apparatus. Metafemur is represented as a 3D-reconstructed model, while the metafemur spring is shown in a light microscopy image. B: Sequential superimposed images illustrating jumping behavior of *As. xanthospilota*. C: Redrawn trajectory depicting the jump path of *As. xanthospilota*.

which were used for genome survey and base error correction. For long-read sequencing, libraries were constructed and sequenced on the Oxford Nanopore Technology (ONT) GridION X5 and PromethION platforms (ONT, UK), generating 93.78 Gb of clean reads for initial assembly of the *As. xanthospilota* genome. These datasets corresponded to estimated genome coverage depths of 102× (Illumina) and 94× (ONT). For high-throughput chromosome conformation capture (Hi-C), mixed male and female samples were sequenced using the Illumina platform (Illumina, USA), generating 86.33 Gb of clean data (88× coverage depth).

Genome assembly: Genome size was estimated using k-mer analysis (k=17). *De novo* assembly was carried out with ONT data using NextDenovo v.2.3.0 (Hu et al., 2024) with default parameters. The initial assembly totaled 1 095.93 Mb and contained 914 contigs. Error correction was performed using Illumina data with purge_dups v.1.2.3 (Guan et al., 2020) and NextPolish v.1.3.1 (Hu et al., 2020), yielding a polished genome of 999.53 Mb. Hi-C clean data were processed using 3D-DNA v.180922 and Juicebox v.2.17.0 (Dudchenko et al., 2017; Durand et al., 2016) to scaffold contigs into pseudo-chromosomes and for visual inspection and error correction. The final chromosome-scale assembly was assessed using Benchmarking Universal Single-Copy Orthologs (BUSCO) v.5.2.2 (Simão et al., 2015) and validated by Hi-C contact heatmap analysis.

Genome annotation: Repeat sequences were predicted and masked using RepeatModeler v.1.73 (Flynn et al., 2020) and RepeatMasker v.4.0.5 (Tarailo-Graovac & Chen, 2009). Transposable elements (TEs), including long terminal repeats (LTRs), tandem repeats, and protein-level elements, were annotated using RepeatMasker, Tandem Repeat Finder v.4.0 (Benson, 1999), RepeatProteinMask v.1.36 (Tarailo-Graovac & Chen, 2009), and *de novo* prediction approaches. Protein-coding genes were annotated using three complementary strategies. (i) *Ab initio* prediction: Gene models were generated *de novo* from the repeat-masked genome using AUGUSTUS v.3.3.3 (Stanke et al., 2006). (ii) Homology-based prediction: Proteome sequences from publicly available genomes were mapped to the *As. xanthospilota* genome using tblastn (blast v.2.2.26) (Altschul et al., 1990) with an E-value cutoff of 1e−5, followed by gene structure modeling with GeneWise v.2.2.0 (Birney et al., 2004). (iii) RNA-seq-based prediction: Total RNA was extracted from whole-body tissues using TRIZOL reagent according to the manufacturer's instructions. RNA quality was assessed via agarose gel electrophoresis. RNA sequencing (RNA-seq) libraries were constructed and sequenced using the Illumina NovaSeq 6000 platform (Illumina, USA). Clean reads were assembled and mapped to the *As. xanthospilota* genome using the PASA v.2.3.3 pipeline (Haas et al., 2008). Gene annotations from the three approaches were integrated using EVidenceModeler v.1.1.1 (Haas et al., 2008).

Gene functional annotation: Predicted protein sequences were functionally annotated by sequence similarity searches against multiple public databases, including NCBI nr (NCBI Resource Coordinators, 2018), SwissProt and TrEMBL (The UniProt Consortium, 2017), Gene Ontology (GO) (Harris et al., 2004), and Kyoto Encyclopedia of Genes and Genomes (KEGG) (Kanehisa & Goto, 2000).

Genome datasets for comparative analysis

High-quality genomes of beetles were retrieved from the NCBI (https://www.ncbi.nlm.nih.gov/) and Ensembl (https://www.ensembl.org/) databases (accessed 23 March 2024) for comparative genomic analysis (Supplementary Table S1). Following established morphological frameworks (Furth & Suzuki, 1992), selected species included jumping beetles and their non-jumping sister taxa from three major families: Chrysomelidae, Curculionidae, and Buprestidae (Supplementary Table S2). Priority was given to chromosome-level assemblies with available genome annotations, although there were a few exceptions. In Buprestidae, no chromosome-level genome with gene annotation was available. Therefore, the scaffold-level genome of *Agrilus planipennis* (Buprestidae: Agrilinae)—the only annotated genome in the family and reported to possess jumping capability (Rodriguez-Soana et al., 2007)—was included. *Dascillus cervinus* (Dascillidae), which has an annotated chromosome-level genome, was also selected as a non-jumping sister lineage of *Agr. planipennis*. In addition, no gene annotations were available for the chromosome-level genome of the jumping weevil *Orchestes rusci* (Curculionidae), so annotation was performed in the present study. In total, six jumping beetles (including *As. xanthospilota*) and six non-jumping sister lineages were

analyzed (Supplementary Table S1). All selected genomes were of relatively high quality (Supplementary Tables S3, S4) and demonstrated >90% completeness for BUSCO insect single-copy orthologs at the protein level.

Two strategies were employed to annotate protein-coding genes in *O. rusci*. Due to the lack of RNA-seq data, both approaches were based on cross-species homology. Repeat sequences were masked using RepeatModeler and RepeatMasker. Homology-based prediction was then performed on the masked genome using miniprot v.0.13, a protein-to-genome alignment tool (Li, 2023). *Ab initio* prediction was carried out using four prediction tools, including AUGUSTUS, GeneMarkES, GlimmerM, and SNAP, implemented via the GenSAS v.6.0 platform (Humann et al., 2019). Gene models generated from both approaches were merged using EVidenceModeler to produce a final integrated annotation set.

Genomic trait comparison

Previous studies have suggested associations between genome-level traits and behavioral adaptations in animals, such as the link between genome or intron size and powered flight (Zhang & Edwards, 2012). To evaluate whether genomic features correlate with jumping ability in beetles, nine genomic traits were compared between jumping and non-jumping taxa. These included genome size (bp), whole-genome GC content, GC content of coding sequences (CDS), mean length of protein-coding genes (kb), mean intron length (kb), mean transcript length (kb, based on pre-mRNA), chromosome count, gene count, and the codon adaptation index (CAI). For *Agr. planipennis*, chromosome count was obtained by averaging values from seven congeneric species (Blackmon & Demuth, 2015). CAI, a measure of codon usage bias (Sharp & Li, 1987), was estimated for each protein-coding gene, and the genome-wide mean was used as a representative measure (Botzman & Margalit, 2011). Prior to interspecies comparison, phylogenetic signal for each genomic trait was quantified using Blomberg's K, estimated via maximum-likelihood (ML) with the package phytools v.2.3.0 (Revell, 2024) in R (v.4.3.2). Based on the strength of phylogenetic signal, differences between jumping and non-jumping beetles were assessed using non-parametric two-tailed Wilcoxon signed-rank test. *P*-values were corrected for multiple testing using the false discovery rate (FDR), with FDR-adjusted $P<0.05$ considered statistically significant.

Orthologous group inference

Orthologous gene groups were inferred using OrthoFinder v2.5.5 (Emms & Kelly, 2019), with DIAMOND v.2.1.12 (Buchfink et al., 2021) used as the underlying sequence similarity search tool and an inflation index of 1.5. To reduce false positives, only the longest isoform of each gene was retained prior to analysis. Based on OrthoFinder outputs, single-copy orthologs (SCOs) were determined as strict 1:1 orthologs present across all studied beetle species, while multi-copy orthologs (MCOs) were defined as 1:N and N:N orthologs (N≥2) present in all taxa.

Phylogenetic analysis

For each SCO gene, amino acid sequences were aligned using MUSCLE v.3.5 (Edgar, 2004), while corresponding protein-coding sequence alignment was performed using PAL2NAL v.14 (Suyama et al., 2006), guided by the amino acid alignments. Ambiguous regions and alignment gaps were excluded using GBlocks v.0.91b with default parameters (Castresana, 2000). Trimmed amino acid alignments were concatenated into a single matrix for phylogenetic inference using ML in IQ-TREE v.1.6.12 (Nguyen et al., 2015). ModelFinder (Kalyaanamoorthy et al., 2017) was used to select the best-fitting substitution model (LG+F+I+G4). Nodal support was assessed via ultrafast bootstrap analysis with 1 000 replicates. In accordance with previous coleopteran phylogenomic studies (Cai et al., 2022; McKenna et al., 2019; Zhang et al., 2018), the species tree was manually rooted at the Elateriformia clade.

To explore potential phylogenetic signals associated with jumping behavior, each SCO gene was tested for fit against two alternative topologies. Tree 1 corresponded to the ML tree, while Tree 2 was a hypothetical topology that grouped all jumping beetles into a single clade, separated from non-jumping taxa. For each gene, the difference in log-likelihood scores (ΔGLS) between Tree 2 and Tree 1 was calculated following Shen et al. (2017). Only genes with aligned amino acid sequences ≥100 residues were included. SCO genes were categorized based on ΔGLS values: those favoring Tree 2 ($\Delta GLS>4$), those favoring Tree 1 ($\Delta GLS<-4$), and genes with no strong preference ($|\Delta GLS|\leq 4$).

Estimation of species divergence times

Divergence times among beetle species were estimated using MCMCTree in PAML v.4.9j (Yang, 2007), with the concatenated amino acid alignment and ML tree as input. Analyses were performed under the independent-rates clock model and approximate likelihood framework, with the Hessian matrix generated via the CodeML module of PAML. The Markov chain Monte Carlo (MCMC) chain was run for 100 000 000 generations, sampled every 5 000 generations to yield 20 000 samples, following a burn-in of 50 000 iterations. To ensure convergence, two independent MCMCTree analyses were performed. Convergence diagnostics, including effective sample size (ESS) for each node age and parameter, were assessed using Tracer v.1.7.2 (Rambaut et al., 2018). All ESS values exceeded 500, indicating robust convergence.

Four fossil calibrations were used to constrain divergence times, based on previously published studies (Cai et al., 2022; Shin et al., 2018; Zhang et al., 2018): (i) root age <293.69 million years ago (Ma); (ii) minimum age of the Curculionoidea-Chrysomeloidea split 155.70 Ma. (iii) Galerucinae divergence <122.50 Ma; and (iv) Curculioninae subfamily age 37.80–98.79 Ma.

Gene family size analysis

Gene family size, defined as the number of gene copies within each family, was analyzed using two approaches. First, expansion and contraction events were inferred using CAFE v.4.2.1 (De Bie et al., 2006) based on OrthoFinder results. A gene family was considered significantly expanded or contracted if the overall family-wide *P*-value was <0.01 and the branch-specific Viterbi *P*-value was <0.05 (De Bie et al., 2006).

Second, to directly test for associations between gene family size and jumping behavior, a phylogenetic generalized linear mixed model was implemented using the "binaryPGLMM()" function in the ape v.5.8 package (Paradis & Schliep, 2019). Copy number of each gene family was tested against binary locomotor classification (jumping versus non-jumping), while accounting for phylogenetic non-independence. Phylogenetic signal for copy number was

assessed via Blomberg's K using phytools. PGLMM was performed with species jumping mode and number of gene members set as the independent variable and predictor, respectively. To control for false positives, a conservative two-model criterion was applied. Results from PGLMM (P<0.05) were cross-validated by Bayesian MCMC generalized linear mixed modeling using the "MCMCglmm()" function in MCMCglmm v2.36 (Hadfield, 2010), with accounting for phylogenetic non-independence. The MCMC chain was run for 100 000 000 generations and sampled every 1 000 generations after discarding 50 000 iterations as burn-in. Convergence and autocorrelation were checked through visual inspection of trace plots. Regression coefficients and P-values were used to assess the relationship between gene family size and jumping behavior. A gene family was considered significantly associated with jumping when both PGLMM and MCMCglmm yielded P-values <0.05; in these cases, a positive coefficient indicated greater copy number in jumping beetles, and a negative coefficient indicated fewer copies. If either P-value exceeded 0.05, the gene family was considered not significantly associated, regardless of effect direction.

Detection of positively selected genes in jumping beetles

To identify genes under positive selection in jumping beetles, the branch-site model in CodeML (PAML) was used. This model detects codon sites with elevated nonsynonymous (d_N) to synonymous (d_S) substitution ratios (ω>1) specifically on foreground branches—in this case, the jumping beetle lineages—while treating all other branches as background. Background sites are modeled as conserved ($0<\omega_0<1$) or neutral ($\omega_1=1$), while a proportion of sites on foreground branches may evolve under positive selection ($\omega_2>1$) (Álvarez-Carretero et al., 2023). Likelihood-ratio tests (LRTs) were performed to compare the alternative model ($\omega_2>1$) with the null model (ω_2 fixed at 1) for each SCO gene. Posterior probabilities of positively selected sites were calculated using the Bayes Empirical Bayes (BEB) method (Zhang et al., 2005). To reduce false positives from alignment errors, three stringent filtering criteria were applied, following previous studies (Li et al., 2024; Potter et al., 2021): (i) unhalved LRT P-value <0.05; (ii) at least one BEB site with posterior probability>0.5; and (iii) if more than five BEB sites were detected, the median interval between sites must exceed 10.

Identification of rapidly evolving genes in jumping beetles

Rapidly evolving genes were defined as those showing significantly elevated ω (d_N/d_S) ratios in specific lineages of an evolutionary tree (Qi et al., 2023). To identify such genes in jumping beetles compared to non-jumping beetles, the branch model in PAML was applied to SCO genes. The two-ratio model (foreground: jumping; background: non-jumping) was compared with the one-ratio model (uniform ω across all branches) via LRT. A gene was considered rapidly evolving if: (i) the two-ratio model significantly outperformed the one-ratio model (FDR-corrected P<0.05), and (ii) the ω estimate for jumping beetle branches exceeded that for non-jumping branches under the two-ratio model.

Testing for gene convergence in jumping beetles

Gene-level convergence was assessed using CSUBST v.1.4.0 (Fukushima & Pollock, 2023), which calculates the error-corrected convergence rate ω_c by comparing d_N and d_S convergence across branch pairs. This approach controls for phylogenetic noise while maintaining high statistical power (Fukushima & Pollock, 2023). CSUBST was applied to each SCO gene, with jumping beetles designated as foreground branches. Pairwise ω_c values were estimated, and 95% confidence intervals (CIs) were calculated using both normal approximation and bootstrap bias-corrected and accelerated (BCa) methods (1 000 replicates) via the boot v.1.3.31 package. Genes with negative lower bounds in the normal-method-based CIs (11% of SCO genes) were excluded due to high estimation uncertainty. Genes were considered convergent if BCa-method-based 95% CIs exceeded ω_c=1, and significantly convergent if 95% CIs exceeded ω_c=3 (Fukushima and Pollock, 2023). Convergent amino acid sites were defined as instances where identical amino acid substitutions occurred independently in separate jumping beetle lineages, as detected under the "any2spec" criterion in CSUBST.

Statistical analysis

All statistical analyses were conducted in R. Wilcoxon signed-rank tests were performed using the stats v.4.3.2 package. GO enrichment analysis of candidate genes was carried out using DAVID v.6.8 (knowledgebase v.2024q2) (Huang et al., 2009) with default settings. GO terms were considered significant at FDR-adjusted P<0.05.

RESULTS

Genome assembly of *As. xanthospilota*

To generate genomic resources for investigating the basis of jumping adaptation, a chromosome-level genome assembly was produced for *As. xanthospilota* using a combination of Illumina short reads, ONT long reads, and Hi-C sequencing. The final assembly had a total length of 999.80 Mb and a scaffold N50 of 58.34 Mb (Figure 2; Supplementary Table S4). Karyotype analysis of male gonads revealed a diploid number of 21 chromosomes (Figure 2A), consistent with the Hi-C scaffolding results, which anchored 97.66% of the assembled sequences to 21 pseudo-chromosomes (Figure 2B).

A total of 17 382 protein-coding genes were annotated in the final assembly, of which 14 265 (82.1%) received functional support from at least one public protein database (KEGG, nr, SwissProt, TrEMBL, or GO) (Figure 2C). BUSCO analysis indicated that 91.4% of single-copy core genes from Insecta were completely recovered in the predicted proteome, suggesting relatively high assembly completeness. The average gene length was 13.01 kb and the average intron length was 3.17 kb. Repeat elements accounted for 62.29% (622.75 Mb) of the genome, with the long interspersed nuclear elements (LINE) being the most abundant class (Supplementary Table S4).

Phylogenetic reconstruction and genes supporting a jumping beetle clade

To obtain a phylogenetic perspective on jumping behaviors in beetles, an ML phylogenetic tree was reconstructed for all jumping and non-jumping beetles included in this study. The analysis was based on a concatenated amino acid alignment comprising 1 003 415 upgapped positions derived from 2 734 SCO genes shared across all species. The resulting ML phylogeny exhibited strong statistical support, with all internal nodes receiving 100% bootstrap support (Figure 3A). The inferred relationships—specifically, the grouping of (Chrysomelidae + Curculionidae) + (Buprestidae +

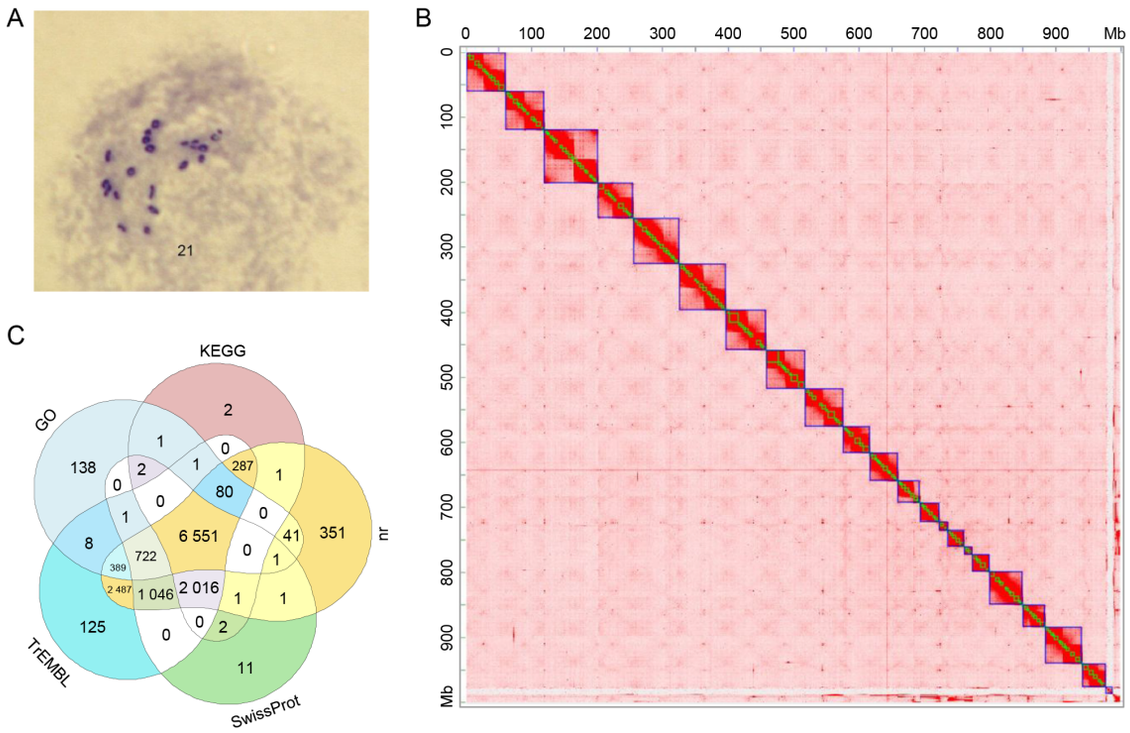

Figure 2 Genome assembly of the flea beetle *Asiophrida xanthospilota*

A: Karyotype analysis showing 21 chromosomes at meiotic prophase I (*n*=21). B: Hi-C contact heatmap (1 Mb resolution). Blue and green squares represent scaffolds and contigs, respectively. C: Venn diagram showing functional annotation of protein-coding genes based on five databases (GO, KEGG, nr, SwissProt, and TrEMBL).

Dascillidae)—were congruent with previous large-scale phylogenomic analyses (Cai et al., 2022; McKenna et al., 2019; Zhang et al., 2018). Divergence time estimates obtained from MCMCTree using four fossil calibration points (Figure 3B) were also broadly concordant with prior estimates, as evidenced by overlapping 95% CIs for deeper nodes across studies (Figure 3B).

To identify potential genes supporting an alternative evolutionary scenario in which jumping beetles form a monophyletic group, each SCO gene was evaluated for its fit to two competing topologies: the reconstructed ML tree (Tree 1) and a hypothetical tree grouping jumping beetles separately from non-jumping lineages (Tree 2). ΔGLS values were computed to quantify support. Nearly all SCO genes (99.8%) favored Tree 1 (ΔGLS<−4), reaffirming the robustness of the species phylogeny (Figure 3C). However, five SCO genes exhibited strong preference for Tree 2 (ΔGLS>4), suggesting localized support for a jumping-associated topology. These included *Rnf185* (ΔGLS=71.28), encoding an E3 ubiquitin-protein ligase, and *Gtf2b* (ΔGLS=44.93), encoding transcription initiation factor IIB (Figure 3C).

Genomic traits and their association with jumping ability in beetles

To assess whether specific genomic features are associated with jumping ability, nine genomic traits were compared between jumping and non-jumping sister lineages (Figure 3D). For all traits, Blomberg's K statistics yielded non-significant *P*-values (*P*=0.08–0.47), indicating limited phylogenetic signal and suggesting that phylogenetic non-independence was unlikely to bias the comparisons. Non-parametric Wilcoxon tests revealed no significant differences in genome size (FDR=0.90) or intron size (FDR=0.40) between jumping and non-jumping groups. Similarly, no significant differences (FDR>0.05) were observed for the remaining seven genomic traits, including genome-wide GC content (FDR=0.57) and codon adaptation index (CAI) (FDR=0.71) (Figure 3D).

Gene family size variation and its association with jumping in beetles

Across the 12 beetle species analyzed, 16 403 orthologous groups (gene families) were identified based on protein-coding gene clustering. Total gene family sizes, defined as the cumulative number of gene copies across species, ranged from 2 to 246 with an average of 11. Using the CAFE framework, significant gene family expansions and contractions were detected along jumping beetle branches (family-wide *P*<0.01, branch-specific *P*<0.05). At the ancestral node of the four flea beetles in Chrysomelidae, 23 gene families exhibited significant expansion and six exhibited significant contraction. In *O. rusci* (Curculionidae), 206 expansions and 11 contractions were observed, while *Agr. planipennis* (Buprestidae) exhibited 15 expansions and 18 contractions. No gene family expansion or contraction was shared across all jumping beetle branches.

To assess whether variation in gene family size correlated with jumping ability, gene copy number across species was tested against locomotor mode (jumping vs. non-jumping) using both binary PGLMM and MCMCglmm while accounting for phylogenetic structure. A total of 24 gene families showed significant associations with jumping, including 14 positively associated and 10 negatively associated (Figure 4A; Supplementary Table S5). Among these, the muscle-related gene *Fhl2*, encoding four and a half LIM domains protein 2-like, exhibited strong positive associations with jumping mode (PGLMM and MCMCglmm regression coefficient >2,

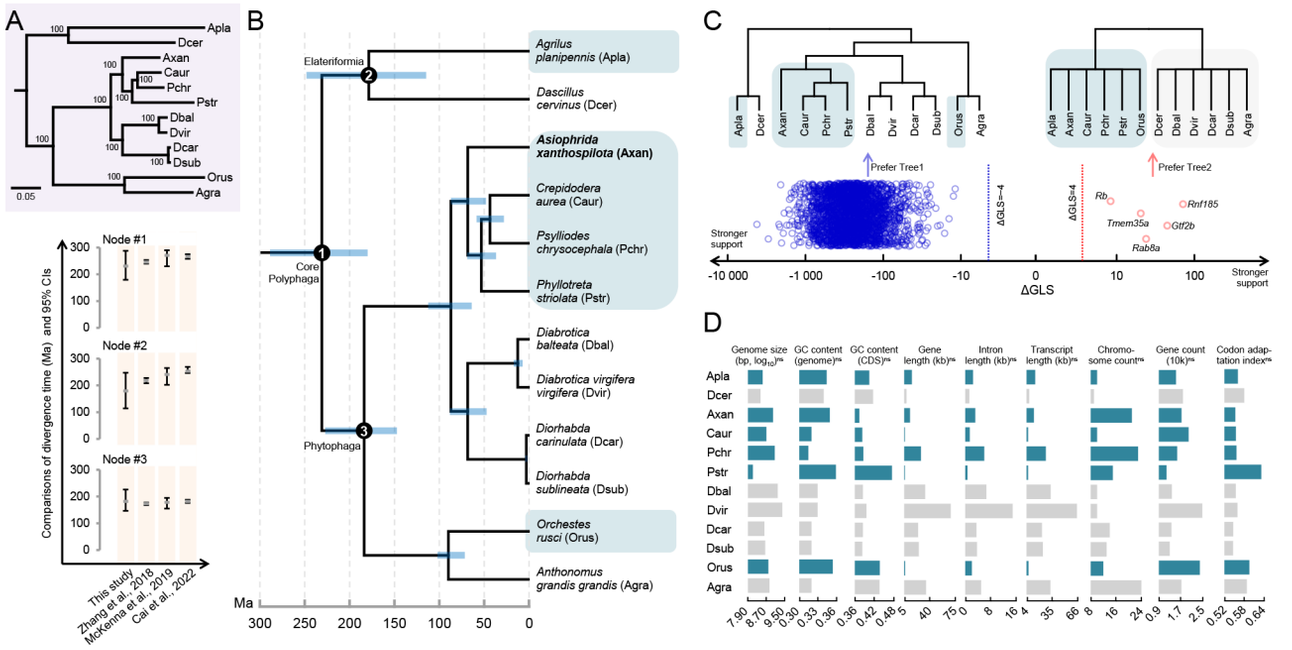

Figure 3 Phylogenetic relationships and genomic trait comparisons between jumping and non-jumping beetles

A: Maximum-likelihood phylogeny inferred from 1 003 415 concatenated amino acid sites. Node values indicate bootstrap support (percentages). Scale bar represents amino acid substitutions per site. B: Time-calibrated phylogeny of studied beetles. Jumping taxa are shaded in light blue; non-jumping taxa are unshaded. *Asiophrida xanthospilota*, sequenced in this study, is indicated in bold. Horizontal bars at nodes represent 95% confidence intervals (CIs). Black circled numbers mark three nodes used for divergence time comparisons (left bottom panel). Ma: Million years ago. C: Topology preference test of single-copy orthologous (SCO) genes based on difference in log-likelihood scores (ΔGLS). Phylogenies show jumping (light blue shading) and non-jumping (unshaded) beetles. Blue circles indicate genes showing stronger support (ΔGLS<−4) for "real" tree topology (left panel, Tree 1); red circles indicate genes showing stronger support (ΔGLS>4) for alternative tree topology (right panel, Tree 2) with a jumping/non-jumping split. Gene names are shown for five genes supporting Tree 2 over Tree 1. D: Comparisons of nine genomic traits between jumping (aqua green) and non-jumping (gray) beetles. Transcript length refers to pre-mRNA. "ns" indicates non-significant difference (Wilcoxon test FDR-adjusted *P*>0.05). CDS: Coding sequence.

P<5.0e−03). Jumping beetles possessed a higher number of *Fhl2* gene copies (2–4) compared to non-jumping lineages (1–2) (Figure 4B). Phylogenetic analysis of Fhl2 protein sequences from the studied beetles and selected animals (e.g., humans and mice) (Supplementary Table S6) recovered a well-supported beetle-specific clade (bootstrap=99%) (Figure 4C). The phylogenetic tree also suggested that the identified beetle Fhl2 proteins were split into two groups, albeit with poor or moderate support (bootstrap=54% and 77%) (Figure 4C).

Rapidly evolving and positively selected genes in jumping beetles

Among the 2 734 SCOs analyzed, 130 genes (4.75%) exhibited signatures of rapid evolution (FDR<0.05) in the six jumping beetle species (Figure 5A; Supplementary Table S7). GO enrichment analysis indicated an overrepresentation of terms related to ATP binding and stress fiber formation, although only the former reached statistical significance after multiple-testing correction (Figure 5A). Complementary tests for positive selection, based on LRT (*P*<0.05) followed by additional *post-hoc* filtering, identified 68 SCO genes (2.5%) under positive selection in jumping beetles (Figure 5A; Supplementary Table S8). However, no GO term reached enrichment significance for this subset, likely reflecting limited statistical power due to the relatively small number of positively selected genes.

Genes involved in energy metabolism, particularly ATP synthesis and transport, displayed widespread signals of rapid evolution and positive selection. Notably, *Acsl6*, which encodes long-chain-fatty-acid-CoA ligase 6 involved in fatty acid metabolism, showed elevated evolutionary rates in jumping beetles (FDR=0.02) compared to non-jumping beetles. Furthermore, three ATP-binding cassette genes—*Abcb8* (FDR=1.73e−03), *Abcf2* (FDR=2.85e−11), and *Abcg4* (FDR=0.04)—also evolved more rapidly in these taxa. Significant rapid evolution and positive selection signals were also detected in genes involved in oxidative phosphorylation, the primary pathway for ATP generation. Using *Agr. planipennis* as a reference mapped in the KEGG database, orthologous genes participating in oxidative phosphorylation were identified by intersecting KEGG annotations with orthogroups defined by OrthoFinder, retaining only those present in all 12 beetle species. Fourteen SCOs and 19 MCOs were mapped to this pathway. Among the SCOs, *Ndufa10* (FDR=1.82e−03), encoding a subunit of NADH dehydrogenase, displayed rapid evolution. Among the MCOs, one positively selected gene *Atp5f1a* (encoding F-type ATPase subunit) and four rapidly evolving genes (*Atp5b*, *Atp5j*, *Atp6g*, and *Atp6m*) encoding F-type and V-type ATPase subunits were identified in the jumping beetle branches (Figure 5A).

In addition to metabolic genes, several muscle-associated genes showed strong evidence of adaptive evolution. These included rapidly evolving genes such as *Obscn* (FDR=0.045), encoding obscurin; *Capza* (FDR=2.63e−03), encoding F-actin-capping protein subunit alpha; and *CG14535* (FDR=1.67e−09), encoding kinesin-like motor protein. Stress

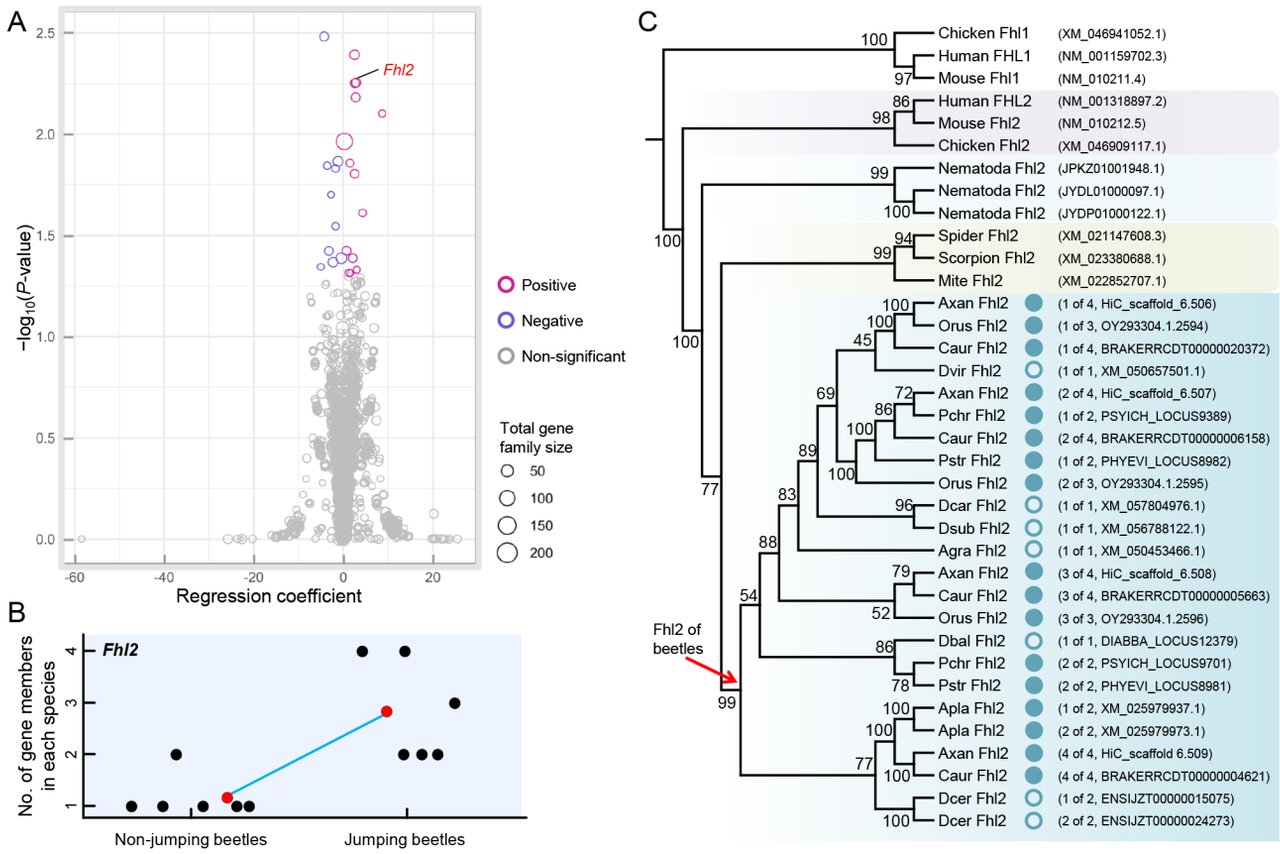

Figure 4 Association between gene family size and jumping ability in beetles

A: Binary phylogenetic generalized linear mixed model (PGLMM) analysis testing gene family size against jumping ability across beetles. Each point represents a gene family; point size reflects total gene count across the 12 species. Red, blue, and gray indicate positive, negative, and non-significant associations, respectively. All significant associations were verified by MCMCglmm. A muscle-related gene (*Fhl2*) is highlighted. B: Comparison of *Fhl2* copy number between jumping and non-jumping beetles. Each point represents a species; red points represent group means. C: Maximum-likelihood phylogenetic tree of *Fhl2* protein sequences from beetles and representative vertebrates (human, mouse, chicken). Solid circles mark jumping beetle sequences; open circles indicate non-jumping beetle sequences. Sequence abbreviations match those in Figure 3. Sequence identifiers and species-specific *Fhl2* copy numbers are provided in parentheses in the format "1 of 4", indicating the current and total copies. For full details, see Supplementary Table S6.

fiber-related genes such as *Pxn* (FDR=0.03), *Zasp52* (FDR=0.04), and *Trip6* (FDR=0.02) also exhibited elevated rates of evolution (Figure 5A). Integration of positive selection and rapid evolution analyses identified four genes, *Dnai4*, *Wdr59*, *Med12*, and *Stk10*, as both rapidly evolving and positively selected (Figure 5A). Notably, *Dnai4*, which encodes dynein axonemal intermediate chain 4, showed exceptionally strong signals (positive selection *P*=1.00e−12, rapid evolution FDR=1.41e−03), implicating its potential role in muscular adaptation for jumping.

Gene convergence associated with jumping behavior in beetles

Convergent evolution has long been proposed as a mechanism underlying the independent emergence of jumping behavior in distinct beetle lineages. To evaluate gene-level convergence, CSUBST was applied to calculate pairwise ω_c values, with convergence inferred when the 95% CIs of ω_c exceeded 1. Based on this criterion, 506 SCO genes exhibited signatures of convergence. Among these, two genes—*xP2* and *bab1*—met the stricter threshold of statistical support (ω_c 95% CIs>3), representing 0.4% of all SCO genes analyzed (Figure 5B). Convergent evolution in *xP2* (mean ω_c=4.79, 95% CI=3.35–6.71) and *bab1* (mean ω_c=6.42, 95% CI=3.06–10.83) was detected across multiple pairwise comparisons among the six jumping beetles (14 non-sister combinations). *xP2* encodes a skin secretory protein xP2-like, while *bab1* encodes bric-à-brac 1-like, a transcription factor involved in leg disc morphogenesis. On average, 15 and 11 convergent amino acid sites were identified in xP2 and bab1, respectively. The specific sites of convergence differed among jumping beetle pairs for both genes, consistent with a "same-gene-different-site" model of molecular convergence previously reported in other taxa (Eliason et al., 2023; Natarajan et al., 2016).

DISCUSSION

Comparative genomic analysis of jumping beetles and their non-jumping sister taxa revealed widespread but selective evolutionary signals in genes associated with basic biological functions, particularly energy metabolism and muscle physiology. These results suggest that the emergence of jumping ability in beetles likely reflects a complex, polygenic adaptation shaped by multiple evolutionary mechanisms. Signatures of adaptation were detected in multiple distinct forms, including positive selection, rapid evolution, gene family expansion or contraction, and gene-level convergence, underscoring the multifaceted nature of this locomotor

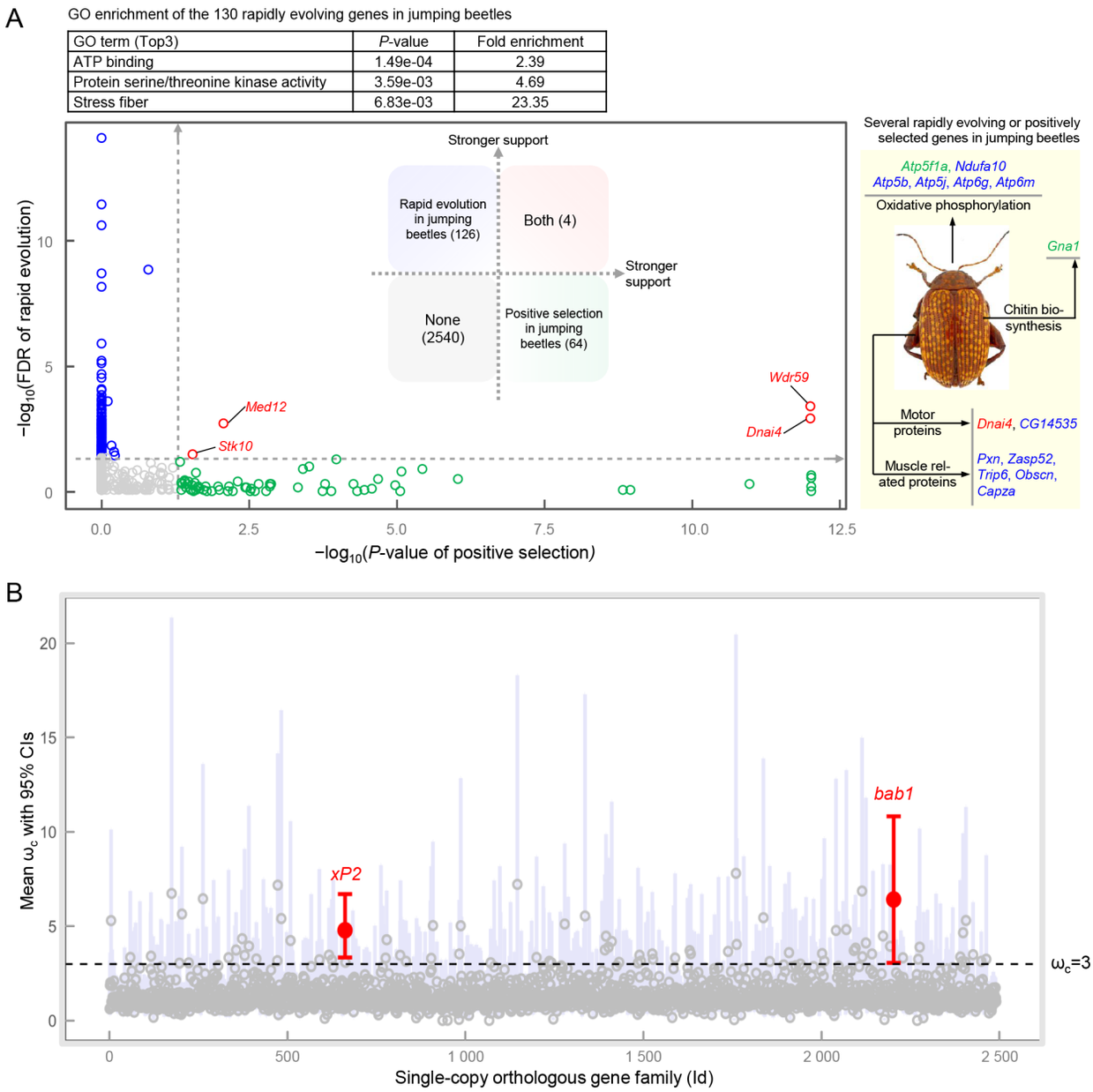

Figure 5 Rapid evolution, positive selection, and gene convergence in six jumping beetles

A: Identification of rapidly evolving and positively selected genes. Blue points represent rapidly evolving genes (FDR<0.05); green points represent positively selected genes (*P*<0.05 after filtering); red points indicate genes under both rapid evolution and positive selection (four genes). Gray points indicate genes lacking either signature. Top sub-panel: GO enrichment analysis of 130 rapidly evolving genes in jumping beetles. Right sub-panel: Rapidly evolving or positively selected genes associated with oxidative phosphorylation, chitin metabolism, and muscle functions (including motor protein) in jumping beetles. Blue, green, and red labels denote rapid evolution, positive selection, and overlap between both, respectively. B: Detection of gene convergence. Mean convergence metric ω_c across 14 species pairs among six jumping beetles (excluding one sister pair). Error bar represents 95% confidence intervals (CIs) calculated by bootstrap approach. Genes with 95% CI exceeding 3 (dashed line) were considered significantly convergent (red). Gene names (*xP2* and *bab1*) are indicated for these cases.

innovation. Notably, irrespective of the signature type concerned, the overall proportion of affected genes remained relatively low. Across the 2 734 SCOs analyzed, the fraction of implicated genes ranged from 0.07% (gene convergence, two genes) to 4.75% (rapidly evolving, 130 genes). This contrasts sharply with previous studies of other locomotor adaptations, such as insect flight, where 13.2% of 954 genes showed signatures of positive selection (Mitterboeck et al., 2017). One possible explanation is that jumping represents a more specialized and anatomically constrained behavior than flight, exerting selective pressure on a narrower set of genomic targets. Among the genes with robust evolutionary signals, those associated with energy metabolism, leg development, and muscle function emerged as key contributors to the evolution of jumping in beetles.

Adaptive evolution of energy metabolism-related genes in jumping beetles

Jumping in beetles is energetically expensive. Molecular evolutionary analyses revealed significant enrichment of rapidly evolving genes associated with ATP-related functions in jumping lineages (Figure 5A). Among these, *Abcg4* and

Abcb8 encode transporters involved in glucose-stimulated insulin secretion (Hou et al., 2016) and mitochondrial iron-sulfur cluster biogenesis, respectively—key processes in maintaining mitochondrial electron transport and ATP production (Read et al., 2021; Zutz et al., 2009). More importantly, several F-type and V-type ATPase subunit genes involved in oxidative phosphorylation also exhibited signatures of both rapid evolution and positive selection. Given that oxidative phosphorylation generates over 95% of cellular ATP in eukaryotes (Erecińska & Wilson, 1982), these results suggest a molecular response to the energetic demands of explosive locomotion in beetles.

This pattern mirrors earlier reports of convergent adaptive evolution in oxidative phosphorylation genes in other high-energy-demand taxa, such as bats (Shen et al., 2010) and flying insects (Mitterboeck et al., 2017). Although both flight and jumping require substantial energy, the underlying biomechanical mechanisms and energy utilization strategies differ. In flea beetles and many other jumping taxa, energy is first stored mechanically within elastic protein-chitin complexes and released explosively via catapult-like systems (Betz et al., 2007; Furth et al., 1983; Furth & Suzuki, 1992). In contrast, sustained wing-beat flight relies on continuous ATP generation from carbohydrate and lipid metabolism (Chatterjee & Perrimon, 2021). Despite this mechanistic divergence, shared evolutionary signals in conserved energy pathways such as oxidative phosphorylation may reflect a common selective pressure to enhance energy metabolism in taxa with energetically costly locomotor behaviors. The consistent association between elevated metabolic expenditure and specialized locomotor strategies supports the hypothesis that metabolic efficiency constitutes a key axis of adaptive evolution (Reinhold, 1999). These results suggest that beetle jumping may serve as a model for uncovering genomic correlates of energy-intensive behaviors more broadly (e.g. Zong et al., 2024), including running, swimming, and walking, where similar evolutionary pressures on ATP production and utilization are likely to operate.

Adaptive evolution of leg development- and muscle-related genes in jumping beetles

Genes involved in leg morphogenesis and muscle function exhibited signatures of convergent evolution in jumping beetles, consistent with the morphological and biomechanical innovations required for high-energy propulsion (Betz et al., 2007; Furth & Suzuki, 1992). Among over 2 000 SCO genes, only two—*bab1* and *xP2*—showed significant convergence in jumping beetles (Figure 5B). Notably, *bab1* is reported to be necessary for leg disc development, and its mutations affect homologous structures in *Drosophila* (Godt et al., 1993). Its evolutionary shift in beetles may underlie developmental modifications that gave rise to the metafemoral spring, a specialized structure housed in hypertrophied legs of many jumping taxa (Furth & Suzuki, 1992). The second convergently evolved gene, *xP2*, encodes a secreted protein originally described as a skin protein with unknown function (Hauser et al., 1992), but later proposed to be involved in protection against natural enemies (Hauser et al., 1992) and recently suggested to belong to the cuticle protein family (Ramsey et al., 2022). Given that the metafemoral spring in the legs of flea beetles comprises cuticle-derived components (Furth et al., 1983; Furth & Suzuki, 1992), functional shifts in xP2 may relate to cuticle reinforcement and mechanical resilience in the context of elastic energy storage.

For muscle, the force and motions to contract are mainly generated by motor proteins dynein, kinesin, and myosin, among which dynein and kinesin use microtubules whereas myosin use actin cytoskeletons to perform functions (Ali & Yang, 2020; Milisav, 1998; Vale & Milligan, 2000). We found that multiple motor protein genes underwent positive selection or rapid evolution in jumping beetles. *Dnai4* (also known as *Wdr78*), which showed signatures of both rapid evolution and positive selection, participates in ciliary movement and axonemal dynein assembly (Braschi et al., 2022; Zhang et al., 2019). The kinesin family gene *CG14535* also showed accelerated evolution, along with three actin-associated genes: *Pxn*, *Zasp52*, and *Trip6*, which contribute to actin-membrane anchorage (Warner et al., 2011), myofibril architecture (Liao et al., 2016), and cytoskeletal remodeling (Lin & Lin, 2011; Ray et al., 2024), respectively. Their evolutionary divergence suggests strong selective pressures on muscle dynamics and actin-based contractility, aligning with the demands of high-powered jumps.

Gene family analysis further revealed a significant expansion of *Fhl2* in jumping beetles after accounting for phylogenetic non-independence (Figure 4). This gene, also known as skeletal muscle LIM-protein 3, plays multiple roles in sarcomere integrity, cytoskeletal organization, and energy coordination in muscle tissue (Johannessen et al., 2006). Fhl2 binds actin filaments, α-actinin, and titin, and has been shown to modulate mechanical stabilization of muscle cells and passive elasticity through interaction with the titin N2B unique sequence, a spring-like element that regulates sarcomere stiffness (Johannessen et al., 2006; Sun et al., 2024). Additionally, Fhl2 functions as a metabolic adaptor, linking to enzymes involved in ATP generation during muscle contraction (Lange et al., 2002). Given these, the elevated copy number of *Fhl2* in jumping beetles may reflect an adaptive genomic amplification supporting increased contractile demand and energetic throughput during explosive locomotion. Although two Elateriformia species exhibited identical *Fhl2* copy numbers regardless of jumping ability, and non-jumping beetles in Chrysomelidae and Curculionidae typically carried fewer copies (one vs. 2–4 and one vs. three, respectively), the limited taxonomic sampling (10 species across eight genera) precludes definitive conclusions. Further lineage-wide comparisons are needed to assess whether *Fhl2* expansion constitutes a general feature of jumping beetles.

Other evolutionary patterns

Five genes exhibited stronger support for an alternative tree topology that showed a split between jumping and non-jumping beetles (Figure 3C). Although these genes did not display significant signatures of positive selection or convergence, partial overlap was observed with the set of rapidly evolving genes identified in this study. Among them, *Rnf185*, which showed the strongest support for the alternative topology, encodes a protein that interacts with paxillin (*Pxn*)—a rapidly evolving actin-associated protein in jumping beetles—and modulates its function by regulating its stability and subcellular localization (Iioka et al., 2007). Possible explanations for the topological discordance include incomplete lineage sorting, hybridization, and methodological artifacts (Shen et al., 2017). Prior studies have also linked genomic features such as intron size to animal behavior; for example, volant birds possess shorter introns than their

flightless relatives (Zhang & Edwards, 2012). A similar, though non-significant, reduction in intron length was observed in jumping beetles relative to non-jumping taxa (Figure 3D), warranting further investigation.

CONCLUSION

This study generated a chromosome-level genome assembly for *As. xanthospilota*, a representative of flea beetles known for exceptional jumping performance. Comparative genomic analysis of *As. xanthospilota*, other jumping beetles from Chrysomelidae, Curculionidae, and Buprestidae, and their non-jumping relatives revealed diverse genomic signatures associated with the evolution of jumping behavior. Genes involved in energy metabolism—particularly oxidative phosphorylation—showed signals of accelerated evolution or positive selection, consistent with the high energetic demands of jumping. Additionally, convergent evolution, adaptive sequence changes, and gene family expansions were detected in muscle (motor) protein genes and leg development regulators, implicating these pathways in the evolution of jumping capacity in beetles.

This study has several limitations that should be noted. First, functional validation was not performed due to the long life cycle (one generation per year) and difficulties in laboratory maintenance of the wild, non-model insect *As. xanthospilota*. Future efforts incorporating functional multi-omics analyses, such as transcriptomic and proteomic profiling, will be essential for validating the functional significance of candidate genes, including *bab1*, *Dnai4*, and *Fhl2*. Second, this study focused on a limited number of jumping beetle lineages. Therefore, the genomic signatures and candidate genes identified may not capture the full diversity of mechanisms underlying jumping in beetles. Broader sampling of jumping taxa in future genomic and functional investigations will provide deeper insights into the molecular basis of this complex locomotor adaptation.

Collectively, these findings underscore the utility of comparative genomics in exploring the evolutionary and mechanistic basis of convergent locomotor traits in insects and lay the groundwork for future studies of jumping behavior across a broader phylogenetic spectrum.

DATA AVAILABILITY

The genome sequencing data of *Asiophrida xanthospilota* have been deposited in the NCBI database (SAMN44272422, BioProjectID PRJNA1172453), GSA database (https://ngdc.cncb.ac.cn/gsa/) (PRJCA044009), and Science Data Bank (doi: 10.57760/sciencedb.j00139.00247).

SUPPLEMENTARY DATA

Supplementary data to this article can be found online.

COMPETING INTERESTS

The authors declare that they have no competing interests.

AUTHORS' CONTRIBUTION

W.W.: Conceptualization, Formal analysis, Methodology, Investigation, Visualization, Writing – original draft, Writing – review & editing. L.Z.: Conceptualization, Formal analysis, Investigation, Visualization, Data curation, Writing – review & editing. J.W.H.: Formal analysis, Investigation, Writing – review & editing. C.Y.M.: Formal analysis, Investigation. Z.W.D.: Formal analysis, Investigation. P.P.Y.: Investigation, Visualization. Z.Z.H.: Investigation, Resource. C.Q.L.: Investigation, Resource. W.J.L.: Investigation, Resource. Y.Y.R.: Resource, Visualization. C.F.: Investigation, Resource. X.Y.L.: Conceptualization, Supervision, Resources, Writing – review & editing, Funding acquisition. S.Q.G.: Conceptualization, Supervision, Data curation, Resources, Writing – review & editing, Funding acquisition. All authors read and approved the final version of the manuscript.

ACKNOWLEDGMENTS

We thank Prof. Wen Wang (Northwestern Polytechnical University) and Prof. De-Xing Zhang (Institute of Zoology Chinese Academy of Sciences) for their support in computational resources. We thank Prof. Yan-Hua Qu (Institute of Zoology Chinese Academy of Sciences) for valuable comments on the manuscript. We thank Dr. Jian Duan (USDA-ARS, USA) for kind permission to use the *Agrilus planipennis* genome annotation.

REFERENCES

Ali I, Yang WC. 2020. The functions of kinesin and kinesin-related proteins in eukaryotes. *Cell Adhesion & Migration*, **14**(1): 139–152.

Altschul SF, Gish W, Miller W, et al. 1990. Basic local alignment search tool. *Journal of Molecular Biology*, **215**(3): 403–410.

Álvarez-Carretero S, Kapli P, Yang ZH. 2023. Beginner's guide on the use of PAML to detect positive selection. *Molecular Biology and Evolution*, **40**(4): msad041.

Benson G. 1999. Tandem repeats finder: a program to analyze DNA sequences. *Nucleic Acids Research*, **27**(2): 573–580.

Betz O, Wegst U, Weide D, et al. 2007. Imaging applications of synchrotron X-ray phase-contrast microtomography in biological morphology and biomaterials science. I. General aspects of the technique and its advantages in the analysis of millimetre-sized arthropod structure. *Journal of Microscopy*, **227**(Pt 1): 51–71.

Birney E, Clamp M, Durbin R. 2004. GeneWise and genomewise. *Genome Research*, **14**(5): 988–995.

Blackmon H, Demuth JP. 2015. Coleoptera karyotype database. *The Coleopterists Bulletin*, **69**(1): 174–175.

Botzman M, Margalit H. 2011. Variation in global codon usage bias among prokaryotic organisms is associated with their lifestyles. *Genome Biology*, **12**(10): R109.

Braschi B, Omran H, Witman GB, et al. 2022. Consensus nomenclature for dyneins and associated assembly factors. *Journal of Cell Biology*, **221**(2): e202109014.

Buchfink B, Reuter K, Drost HG. 2021. Sensitive protein alignments at tree-of-life scale using DIAMOND. *Nature Methods*, **18**(4): 366–368.

Cai CY, Tihelka E, Giacomelli M, et al. 2022. Integrated phylogenomics and fossil data illuminate the evolution of beetles. *Royal Society Open Science*, **9**(3): 211771.

Castresana J. 2000. Selection of conserved blocks from multiple alignments for their use in phylogenetic analysis. *Molecular Biology and Evolution*, **17**(4): 540–552.

Chapman RF. 2013. The Insects: Structure and Function. 5th ed. Cambridge: Cambridge University Press.

Chatterjee N, Perrimon N. 2021. What fuels the fly: energy metabolism in *Drosophila* and its application to the study of obesity and diabetes. *Science Advances*, **7**(24): eabg4336.

De Bie T, Cristianini N, Demuth JP, et al. 2006. CAFE: a computational tool for the study of gene family evolution. *Bioinformatics*, **22**(10): 1269–1271.

Douglas HB, Konstantinov AS, Brunke AJ, et al. 2023. Phylogeny of the flea beetles (Galerucinae: Alticini) and the position of *Aulacothorax* elucidated through anchored phylogenomics (Coleoptera: Chrysomelidae: Alticini). *Systematic Entomology*, **48**(3): 361–386.

Dudchenko O, Batra SS, Omer AD, et al. 2017. *De novo* assembly of the *Aedes aegypti* genome using Hi-C yields chromosome-length scaffolds. *Science*, **356**(6333): 92–95.

Durand NC, Robinson JT, Shamim MS, et al. 2016. Juicebox provides a visualization system for Hi-C contact maps with unlimited zoom. *Cell*

Systems, **3**(1): 99–101.
Eastment RV, Wong BBM, McGee MD. 2024. Convergent genomic signatures associated with vertebrate viviparity. *BMC Biology*, **22**(1): 34.
Edgar RC. 2004. MUSCLE: multiple sequence alignment with high accuracy and high throughput. *Nucleic Acids Research*, **32**(5): 1792–1797.
Eliason CM, Mellenthin LE, Hains T, et al. 2023. Genomic signatures of convergent shifts to plunge-diving behavior in birds. *Communications Biology*, **6**(1): 1011.
Emms DM, Kelly S. 2019. OrthoFinder: phylogenetic orthology inference for comparative genomics. *Genome Biology*, **20**(1): 238.
Erecińska M, Wilson DF. 1982. Regulation of cellular energy metabolism. *The Journal of Membrane Biology*, **70**(1): 1–14.
Flynn JM, Hubley R, Goubert C, et al. 2020. RepeatModeler2 for automated genomic discovery of transposable element families. *Proceedings of the National Academy of Sciences of the United States of America*, **117**(17): 9451–9457.
Fukushima K, Pollock DD. 2023. Detecting macroevolutionary genotype-phenotype associations using error-corrected rates of protein convergence. *Nature Ecology & Evolution*, **7**(1): 155–170.
Furth DG, Suzuki K. 1992. The independent evolution of the metafemoral spring in Coleoptera. *Systematic Entomology*, **17**(4): 341–349.
Furth DG, Traub W, Harpaz I. 1983. What makes *Blepharida* jump? A structural study of the metafemoral spring of a flea beetle. *Journal of Experimental Zoology*, **227**(1): 43–47.
Ge DY, Chesters D, Gómez-Zurita J, et al. 2011. Anti-predator defence drives parallel morphological evolution in flea beetles. *Proceedings of the Royal Society B: Biological Sciences*, **278**(1715): 2133–2141.
Godt D, Couderc JL, Cramton SE, et al. 1993. Pattern formation in the limbs of *Drosophila: bric à brac* is expressed in both a gradient and a wave-like pattern and is required for specification and proper segmentation of the tarsus. *Development*, **119**(3): 799–812.
Guan DF, McCarthy SA, Wood J, et al. 2020. Identifying and removing haplotypic duplication in primary genome assemblies. *Bioinformatics*, **36**(9): 2896–2898.
Haas BJ, Salzberg SL, Zhu W, et al. 2008. Automated eukaryotic gene structure annotation using EVidenceModeler and the Program to Assemble Spliced Alignments. *Genome Biology*, **9**(1): R7.
Hadfield JD. 2010. MCMC methods for multi-response generalized linear mixed models: the MCMCglmm R package. *Journal of Statistical Software*, **33**(2): 1–22.
Hao Y, Qu YH, Song G, et al. 2019. Genomic insights into the adaptive convergent evolution. *Current Genomics*, **20**(2): 81–89.
Harris MA, Clark J, Ireland A, et al. 2004. The Gene Ontology (GO) database and informatics resource. *Nucleic Acids Research*, **32**(S1): D258–D261.
Hauser F, Roeben C, Hoffmann W. 1992. xP2, a new member of the P-domain peptide family of potential growth factors, is synthesized in *Xenopus laevis* skin. *Journal of Biological Chemistry*, **267**(20): 14451–14455.
Hou XW, Wu W, Yin B, et al. 2016. MicroRNA-463-3p/ABCG4: a new axis in glucose-stimulated insulin secretion. *Obesity*, **24**(11): 2368–2376.
Hu J, Fan JP, Sun ZY, et al. 2020. NextPolish: a fast and efficient genome polishing tool for long-read assembly. *Bioinformatics*, **36**(7): 2253–2255.
Hu J, Wang Z, Sun ZY, et al. 2024. NextDenovo: an efficient error correction and accurate assembly tool for noisy long reads. *Genome Biology*, **25**(1): 107.
Hu YB, Wu Q, Ma S, et al. 2017. Comparative genomics reveals convergent evolution between the bamboo-eating giant and red pandas. *Proceedings of the National Academy of Sciences of the United States of America*, **114**(5): 1081–1086.
Huang DW, Sherman BT, Lempicki RA. 2009. Systematic and integrative analysis of large gene lists using DAVID bioinformatics resources. *Nature Protocols*, **4**(1): 44–57.
Humann JL, Lee T, Ficklin S, et al. 2019. Structural and functional annotation of eukaryotic genomes with GenSAS. *Methods in Molecular Biology*, **1962**: 29–51.
Iioka H, Iemura SI, Natsume T, et al. 2007. Wnt signalling regulates paxillin ubiquitination essential for mesodermal cell motility. *Nature Cell Biology*, **9**(7): 813–821.
Johannessen M, Møller S, Hansen T, et al. 2006. The multifunctional roles of the four-and-a-half-LIM only protein FHL2. *Cellular and Molecular Life Sciences CMLS*, **63**(3): 268–284.
Kalyaanamoorthy S, Minh BQ, Wong TKF, et al. 2017. ModelFinder: fast model selection for accurate phylogenetic estimates. *Nature Methods*, **14**(6): 587–589.
Kanehisa M, Goto S. 2000. KEGG: Kyoto encyclopedia of genes and genomes. *Nucleic Acids Research*, **28**(1): 27–30.
Krasnov BR, Khokhlova IS, Burdelov SA, et al. 2004. Metabolic rate and jump performance in seven species of desert fleas. *Journal of Insect Physiology*, **50**(2-3): 149–156.
Lange S, Auerbach D, McLoughlin P, et al. 2002. Subcellular targeting of metabolic enzymes to titin in heart muscle may be mediated by DRAL/FHL-2. *Journal of Cell Science*, **115**(Pt 24): 4925–4936.
Li FB, Wang W, Cheng HH, et al. 2024. Genome-wide analysis reveals the contributors to fast molecular evolution of the Chinese hook snout carp (*Opsariichthys bidens*). *Computational and Structural Biotechnology Journal*, **23**: 2465–2477.
Li H. 2023. Protein-to-genome alignment with miniprot. *Bioinformatics*, **39**(1): btad014.
Liao KA, González-Morales N, Schöck F. 2016. Zasp52, a core Z-disc protein in *Drosophila* indirect flight muscles, interacts with α-actinin via an extended PDZ domain. *PLoS Genetics*, **12**(10): e1006400.
Lin VTG, Lin FT. 2011. TRIP6: an adaptor protein that regulates cell motility, antiapoptotic signaling and transcriptional activity. *Cellular Signalling*, **23**(11): 1691–1697.
Maulik S. 1929. On the structure of the hind femur in halticine beetles. *Proceedings of the Zoological Society of London*, **99**(2): 305–308.
McKenna DD, Shin S, Ahrens D, et al. 2019. The evolution and genomic basis of beetle diversity. *Proceedings of the National Academy of Sciences of the United States of America*, **116**(49): 24729–24737.
Milisav I. 1998. Dynein and dynein-related genes. *Cell Motility and the Cytoskeleton*, **39**(4): 261–272.
Mitterboeck TF, Liu SL, Adamowicz SJ, et al. 2017. Positive and relaxed selection associated with flight evolution and loss in insect transcriptomes. *GigaScience*, **6**(10): gix073.
Nadein K, Betz O. 2016. Jumping mechanisms and performance in beetles. I. Flea beetles (Coleoptera: Chrysomelidae: Alticini). *Journal of Experimental Biology*, **219**(Pt 13): 2015–2027.
Nadein K, Betz O. 2018. Jumping mechanisms and performance in beetles. II. Weevils (Coleoptera: Curculionidae: Rhamphini). *Arthropod Structure & Development*, **47**(2): 131–143.
Nadein K, Kovalev A, Gorb SN. 2022. Jumping mechanism in the marsh beetles (Coleoptera: Scirtidae). *Scientific Reports*, **12**(1): 15834.
Natarajan C, Hoffmann FG, Weber RE, et al. 2016. Predictable convergence in hemoglobin function has unpredictable molecular underpinnings. *Science*, **354**(6310): 336–339.
NCBI Resource Coordinators. 2018. Database resources of the National Center for Biotechnology Information. *Nucleic Acids Research*, **46**(D1): D8–D13.
Nguyen LT, Schmidt HA, von Haeseler A, et al. 2015. IQ-TREE: a fast and effective stochastic algorithm for estimating maximum-likelihood phylogenies. *Molecular Biology and Evolution*, **32**(1): 268–274.
Paradis E, Schliep K. 2019. ape 5.0: an environment for modern phylogenetics and evolutionary analyses in R. *Bioinformatics*, **35**(3): 526–528.

Potter JHT, Davies KTJ, Yohe LR, et al. 2021. Dietary diversification and specialization in Neotropical bats facilitated by early molecular evolution. *Molecular Biology and Evolution*, **38**(9): 3864–3883.

Qi XG, Wu JW, Zhao L, et al. 2023. Adaptations to a cold climate promoted social evolution in Asian colobine primates. *Science*, **380**(6648): eabl8621.

Rambaut A, Drummond AJ, Xie D, et al. 2018. Posterior summarization in Bayesian phylogenetics using Tracer 1.7. *Systematic Biology*, **67**(5): 901–904.

Ramsey JS, Ammar ED, Mahoney JE, et al. 2022. Host plant adaptation drives changes in *Diaphorina citri* proteome regulation, proteoform expression, and transmission of "*Candidatus* Liberibacter asiaticus", the citrus greening pathogen. *Phytopathology*, **112**(1): 101–115.

Ray S, DeSilva C, Dasgupta I, et al. 2024. The ability of the LIMD1 and TRIP6 LIM domains to bind strained f-actin is critical for their tension dependent localization to adherens junctions and association with the Hippo pathway kinase LATS1. *Cytoskeleton*, **81**(9-10): 436–447.

Read AD, Bentley RE, Archer SL, et al. 2021. Mitochondrial iron-sulfur clusters: structure, function, and an emerging role in vascular biology. *Redox Biology*, **47**: 102164.

Reinhold K. 1999. Energetically costly behaviour and the evolution of resting metabolic rate in insects. *Functional Ecology*, **13**(2): 217–224.

Revell LJ. 2024. phytools 2.0: an updated R ecosystem for phylogenetic comparative methods (and other things). *PeerJ*, **12**: e16505.

Ribak G, Weihs D. 2011. Jumping without using legs: the jump of the click-beetles (*Elateridae*) is morphologically constrained. *PLoS One*, **6**(6): e20871.

Rodriguez-Soana CR, Miller JR, Poland TM, et al. 2007. Behaviors of adult *Agrilus planipennis* (Coleoptera: Buprestidae). *Great Lakes Entomologist*, **40**(1&2): 1.

Rosenblum EB, Parent CE, Brandt EE. 2014. The molecular basis of phenotypic convergence. *Annual Review of Ecology, Evolution, and Systematics*, **45**: 203–226.

Ruan YY, Konstantinov AS, Shi GY, et al. 2020. The jumping mechanism of flea beetles (Coleoptera, Chrysomelidae, Alticini), its application to bionics and preliminary design for a robotic jumping leg. *ZooKeys*, **915**: 87–105.

Sadanandan KR, Ko MC, Low GW, et al. 2023. Convergence in hearing-related genes between echolocating birds and mammals. *Proceedings of the National Academy of Sciences of the United States of America*, **120**(43): e2307340120.

Schmitt M. 2004. Jumping flea beetles: structure and performance (Insecta, Chrysomelidae, Alticinae). *In*: Jolivet P, Santiago-Baly JA, Schmitt M. New Developments in the Biology of Chrysomelidae. Hague: SPB Academic Publications, 161–169.

Sharp PM, Li WH. 1987. The codon adaptation index-a measure of directional synonymous codon usage bias, and its potential applications. *Nucleic Acids Research*, **15**(3): 1281–1295.

Shen XX, Hittinger CT, Rokas A. 2017. Contentious relationships in phylogenomic studies can be driven by a handful of genes. *Nature Ecology & Evolution*, **1**(5): 126.

Shen YY, Liang L, Zhu ZH, et al. 2010. Adaptive evolution of energy metabolism genes and the origin of flight in bats. *Proceedings of the National Academy of Sciences of the United States of America*, **107**(19): 8666–8671.

Shin S, Clarke DJ, Lemmon AR, et al. 2018. Phylogenomic data yield new and robust insights into the phylogeny and evolution of weevils. *Molecular Biology and Evolution*, **35**(4): 823–836.

Simão FA, Waterhouse RM, Ioannidis P, et al. 2015. BUSCO: assessing genome assembly and annotation completeness with single-copy orthologs. *Bioinformatics*, **31**(19): 3210–3212.

Smith AA, Harrison JS. 2024. Jumping performance and behavior of the globular springtail *Dicyrtomina minuta*. *Integrative Organismal Biology*, **6**(1): obae029.

Stanke M, Keller O, Gunduz I, et al. 2006. AUGUSTUS: *ab initio* prediction of alternative transcripts. *Nucleic Acids Research*, **34**(S2): W435–W439.

Stern DL. 2013. The genetic causes of convergent evolution. *Nature Reviews Genetics*, **14**(11): 751–764.

Sun YZ, Liu XY, Huang WM, et al. 2024. Structural domain in the Titin N2B-us region binds to FHL2 in a force-activation dependent manner. *Nature Communications*, **15**(1): 4496.

Suyama M, Torrents D, Bork P. 2006. PAL2NAL: robust conversion of protein sequence alignments into the corresponding codon alignments. *Nucleic Acids Research*, **34**(S2): W609–W612.

Tarailo-Graovac M, Chen NS. 2009. Using RepeatMasker to identify repetitive elements in genomic sequences. *Current Protocols in Bioinformatics*, **Chapter 4**: 4.10. 1–4.10. 14.

The UniProt Consortium. 2017. UniProt: the universal protein knowledgebase. *Nucleic Acids Research*, **45**(D1): D158–D169.

Tong C. 2024. Convergent genomics and Arctic adaptation of ruminants. *Proceedings of the Royal Society B: Biological Sciences*, **291**(2014): 20232448.

Vale RD, Milligan RA. 2000. The way things move: looking under the hood of molecular motor proteins. *Science*, **288**(5463): 88–95.

Wan WT, Dong ZW, Li J, et al. 2020. Karyotype analysis of butterflies. ***Bio-101***: e1010646. (in Chinese)

Warner A, Qadota H, Benian GM, et al. 2011. The *Caenorhabditis elegans* paxillin orthologue, PXL-1, is required for pharyngeal muscle contraction and for viability. *Molecular Biology of the Cell*, **22**(14): 2551–2563.

Yang J, Wan WT, Xie M, et al. 2020. Chromosome-level reference genome assembly and gene editing of the dead-leaf butterfly *Kallima inachus*. *Molecular Ecology Resources*, **20**(4): 1080–1092.

Yang PP. 2020. The Jumping Performance and Leg's Functional Morphology of Flea Beetles. Master thesis, Hebei University, Baoding. (in Chinese)

Yang ZH. 2007. PAML 4: phylogenetic analysis by maximum likelihood. *Molecular Biology and Evolution*, **24**(8): 1586–1591.

Zhang JZ, Nielsen R, Yang ZH. 2005. Evaluation of an improved branch-site likelihood method for detecting positive selection at the molecular level. *Molecular Biology and Evolution*, **22**(12): 2472–2479.

Zhang Q, Edwards SV. 2012. The evolution of intron size in amniotes: a role for powered flight? *Genome Biology and Evolution*, **4**(10): 1033–1043.

Zhang SQ, Che LH, Li Y, et al. 2018. Evolutionary history of Coleoptera revealed by extensive sampling of genes and species. *Nature Communications*, **9**(1): 205.

Zhang YR, Chen YW, Zheng JQ, et al. 2019. Vertebrate Dynein-f depends on Wdr78 for axonemal localization and is essential for ciliary beat. *Journal of Molecular Cell Biology*, **11**(5): 383–394.

Zhou J, Zhou XF, Yue HS, et al. 2025. Genomic insights into the convergent evolution of desert adaptation in camels and antelopes. *Zoological Research*, **46**(4): 939–952.

Zong L, Sun ZH, Zhao JL, et al. 2024. A self-locking mechanism of the frog-legged beetle *Sagra femorata*. *Insect Science*, **31**(6): 1864–1875.

Zong L, Wu JN, Yang PP, et al. 2023. Jumping of flea beetles onto inclined platforms. *Journal of Comparative Physiology A*, **209**(2): 253–263.

Zou DH, Huang S, Tian SL, et al. 2024. Comparative genomics sheds new light on the convergent evolution of infrared vision in snakes. *Proceedings of the Royal Society B: Biological Sciences*, **291**(2027): 20240818.

Zutz A, Gompf S, Schägger H, et al. 2009. Mitochondrial ABC proteins in health and disease. *Biochimica et Biophysica Acta (BBA) - Bioenergetics*, **1787**(6): 681–690.